NeuroImage 54 (2011) 2571–2581

Contents lists available at ScienceDirect

NeuroImage

journal homepage: www.elsevier.com/locate/ynimg

Functional segregation of the human cingulate cortex is confirmed by functional connectivity based neuroanatomical parcellation

Chunshui Yu [a,*,1], Yuan Zhou [b,1], Yong Liu [c,1], Tianzi Jiang [c], Haiwei Dong [a], Yunting Zhang [a], Martin Walter [d]

[a] Department of Radiology, Tianjin Medical University General Hospital, Tianjin, China
[b] Center for Social and Economic Behavior, Institute of Psychology, Chinese Academy of Sciences, Beijing, China
[c] LIAMA Center for Computational Medicine, National Laboratory of Pattern Recognition, Institute of Automation, Chinese Academy of Sciences, Beijing, China
[d] Clinical Affective Neuroimaging Laboratory, Department of Psychiatry, Otto von-Guericke University of Magdeburg, Magdeburg, Germany

ARTICLE INFO

Article history:
Received 6 July 2010
Revised 7 October 2010
Accepted 3 November 2010
Available online 10 November 2010

Keywords:
Human brain
Cingulate cortex
Subregions
Functional connectivity
Resting-state
Magnetic resonance imaging

ABSTRACT

The four-region model with 7 specified subregions represents a theoretical construct of functionally segregated divisions of the cingulate cortex based on integrated neurobiological assessments. Under this framework, we aimed to investigate the functional specialization of the human cingulate cortex by analyzing the resting-state functional connectivity (FC) of each subregion from a network perspective. In 20 healthy subjects we systematically investigated the FC patterns of the bilateral subgenual (sACC) and pregenual (pACC) anterior cingulate cortices, anterior (aMCC) and posterior (pMCC) midcingulate cortices, dorsal (dPCC) and ventral (vPCC) posterior cingulate cortices and retrosplenial cortices (RSC). We found that each cingulate subregion was specifically integrated in the predescribed functional networks and showed anti-correlated resting-state fluctuations. The sACC and pACC were involved in an affective network and anti-correlated with the sensorimotor and cognitive networks, while the pACC also correlated with the default-mode network and anti-correlated with the visual network. In the midcingulate cortex, however, the aMCC was correlated with the cognitive and sensorimotor networks and anti-correlated with the visual, affective and default-mode networks, whereas the pMCC only correlated with the sensorimotor network and anti-correlated with the cognitive and visual networks. The dPCC and vPCC involved in the default-mode network and anti-correlated with the sensorimotor, cognitive and visual networks, in contrast, the RSC was mainly correlated with the PCC and thalamus. Based on a strong hypothesis driven approach of anatomical partitions of the cingulate cortex, we could confirm their segregation in terms of functional neuroanatomy, as suggested earlier by task studies or exploratory multi-seed investigations.

Introduction

The human cingulate cortex is a complex central structure implicated in diverse functional domains. One widely accepted theoretical construct of its subdivisions is the four-region model with subregions based on integrated neurobiological assessments (Vogt, 2005). These regions and their subregions are the anterior cingulate cortex (ACC; s, subgenual; p, pregenual), the midcingulate cortex (MCC; a, anterior; p, posterior), the posterior cingulate cortex (PCC; d, dorsal; v, ventral), and the retrosplenial cortex (RSC) (Vogt et al., 1993; Vogt, 2005). Each region represents an aggregate of areas that have similar underlying cytoarchitectural features, common connections and functions as observed in human or primate studies. The construct however strongly relies on anatomical connectivity assumptions that were derived from tracer studies in rodents or non-human primates and on activations in task-based neuroimaging, especially the functional magnetic resonance imaging (fMRI) studies.

The sACC was found to be specifically involved during the memory of negative events and during sadness tasks (George et al., 1995; Kross et al., 2009; Liotti et al., 2000). Whereas the pACC is activated during happy events (Rogers et al., 2004; Rolls et al., 2008; Walter et al., 2008, 2009) and self-relevant tasks (Enzi et al., 2009; Kelley et al., 2002). This important distinction is also represented by different metabolic abnormalities of the two regions in major depression with hyperactivity in the sACC and hypoactivation in the pACC (Walter et al., 2009). The function of aMCC is rather complex and is involved in processing cognitive (Luo et al., 2007; Pourtois et al., 2010; Sohn et al., 2007; Ursu et al., 2009), fear (Vogt, 2005), pain (Vogt, 2005) and complex motor tasks (Paus, 2001; Picard and Strick, 1996, 2001). In contrast, the pMCC was activated during simple motor tasks (Beckmann et al., 2009; Paus, 2001; Picard and Strick, 1996, 2001). In the posterior division, both the PCC and RSC are implicated in memory (Maguire, 2001). However, the functional specialization of each subregion has been shown, specifically, the dPCC in visuospatial orientation (Vogt et al., 2006), the vPCC in self-relevant assessment (Vogt et al., 2006),

* Corresponding author. Department of Radiology, Tianjin Medical University General Hospital, No. 154, Anshan Road, Heping District, Tianjin 300052, China. Fax: +8622 60362990.
E-mail address: chunshuiyu@yahoo.cn (C. Yu).

1053-8119/$ – see front matter © 2010 Elsevier Inc. All rights reserved.
doi:10.1016/j.neuroimage.2010.11.018

and the RSC in episodic memory, navigation, imagination and planning for the future (Vann et al., 2009).

Although the task-based fMRI studies have contributed much to our understanding of functions of the human cingulate cortex, a key limitation to these paradigms is that they cannot distinguish task-related activation in a single network from coactivation of distinct networks (Friston et al., 1996). That is to say, a direct confirmation of the specific connectivity of each cingulate subregion with other specific brain areas or networks remains difficult, since task-based studies are normally sensitive, if not highly specific, to some subfunctions while potentially neglecting other important aspects which would be necessary for an unbiased comparison of connectivities in all partitions. The functional complexity of the cingulate cortex as one region may thus be better accounted for by one measure called resting-state functional connectivity (FC) that equally assesses the level of coactivation of resting-state fMRI time-series between anatomically separated brain regions (van den Heuvel and Pol, 2010). A first attempt that explored the functional diversity of the ACC has been performed by Margulies et al. (2007) who have examined resting-state FC patterns for 16 seed regions systematically placed throughout caudal, rostral, and subgenual ACC in each hemisphere. They found strong indications of both rostral/caudal and dorsal/ventral functional distinctions of the ACC, and highlighted negative relationships between rostral ACC-based affective networks and caudal ACC-based frontoparietal attention networks (Margulies et al., 2007). Recently, Habas (2010) has mapped the FC patterns of the human rostral and caudal cingulate motor areas, and found that the rostral cingulate motor area was more in relation with prefrontal, orbitofrontal, and language-associated cortices, whereas the caudal cingulate motor area more related to sensory cortex (Habas, 2010). However, there is no study focused on the patterns of FCs in terms of the four-region model of the cingulate cortex (Vogt, 2005), which is a basic framework of cingulate subdivisions for understanding the functional specialization of each cingulate subregion.

In the present study, we thus systematically mapped the resting-state FC patterns of the predefined cingulate subregions of the four-region model from a functional network perspective. We aimed to understand the functional specialization of the human cingulate cortex in terms of distinct FC patterns of different cingulate subregions, and to recognize interactions between different brain functional networks by analyzing the negative relationships between functional networks with which each cingulate subregion correlated and anti-correlated. Five brain functional networks were paid special attention. The first is the default-mode network (DMN) including the PCC/precuneus (Pcu), lateral parietal cortex (LPC), medial prefrontal cortex, anterior and medial parts of the superior frontal gyrus (SFG), and anterior part of the middle and inferior temporal gyri (MTG/ITG) (Fox et al., 2005; Fransson, 2005; Greicius et al., 2003). The second is the affective network (AN) including the medial prefrontal cortex (MPFC), orbitofrontal cortex (OFC), and temporal pole (George et al., 1995; Levesque et al., 2003). The third is the sensorimotor network (SMN) including the precentral (PreCG) and postcentral (PostCG) gyri, paracentral lobule (ParaCG), Rolandic area, supplementary motor area (SMA) and premotor area (Hanggi et al., 2010; Keisker et al., 2010). The fourth is the cognitive network (CN) including the dorsolateral prefrontal cortex (DLPFC), ventrolateral prefrontal cortex (VLPFC), and dorsolateral parietal cortex (Seeley et al., 2007). The last one is the visual network (VN) including cuneus, lingual and fusiform gyri, superior (SOG), middle (MOG) and inferior (IOG) occipital gyri (Fink et al., 1997).

Subjects and methods

Subjects

Twenty healthy adults (6 males and 14 females) with a mean age of (40.6 ± 10.7) years, were recruited via advertisement. They were right-handed as evaluated by a questionnaire which designed according to the Edinburgh handedness inventory (Oldfield, 1971). They have never suffered from any psychiatric or neurological diseases, and did not have any contraindications to MRI scan. All subjects signed an informed consent form approved by the local Medical Research Ethics Committee.

MR image acquisition

MR images were acquired on a 3.0 Tesla MR scanner (Magnetom Trio, Siemens, Erlangen, Germany). Foam pads were used to reduce head movements and scanner noise. Resting-state fMRI scans were performed by an echo planar imaging (EPI) sequence with scan parameters of repetition time (TR) = 2000 ms, echo time (TE) = 30 ms, flip angle (FA) = 90°, matrix = 64 × 64, field of view (FOV) = 220 × 220 mm^2, slice thickness = 3 mm, and slice gap = 1 mm. Each brain volume comprised 32 axial slices and each functional run contained 180 volumes. During fMRI scans, all subjects were instructed to keep their eyes closed, relax and move as little as possible. In order to cover the whole cerebral cortex, the cerebellum could not be entirely covered in some participants using the current scan parameters. Thus, the cerebellum was excluded from the following analyses. Sagittal T1-weighted images were also acquired by a magnetization prepared rapid

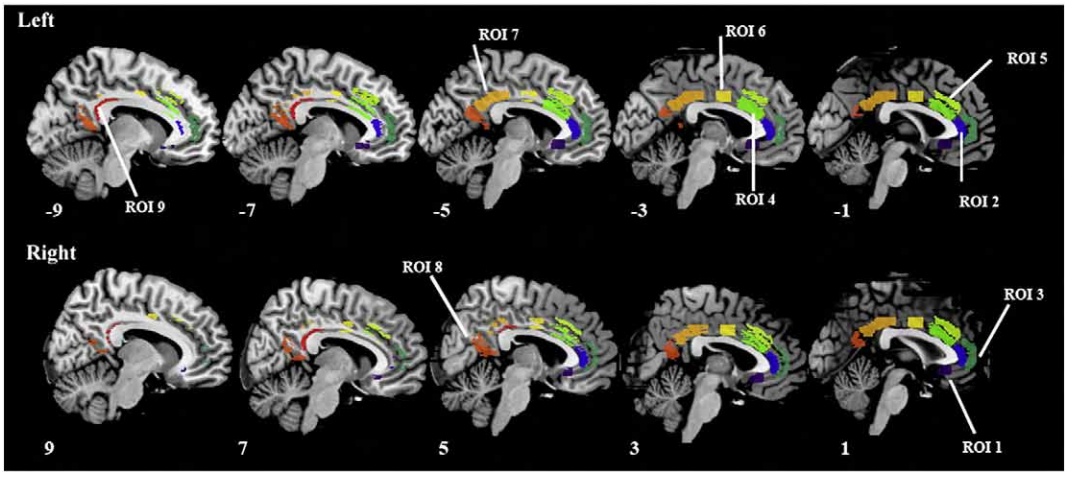

Fig. 1. Regions of interest (ROIs) of the cingulate subregions. ROIs of each side of the cingulate cortex are shown on 10 sagittal anatomical images of the ch2bet template. The positive values (1, 3, 5, 7, 9) of the x-axis coordinates represent the right hemisphere, while the negative values (−1, −3, −5, −7, −9) denote the left hemisphere. Each color represents a ROI, which is labeled in the figure.

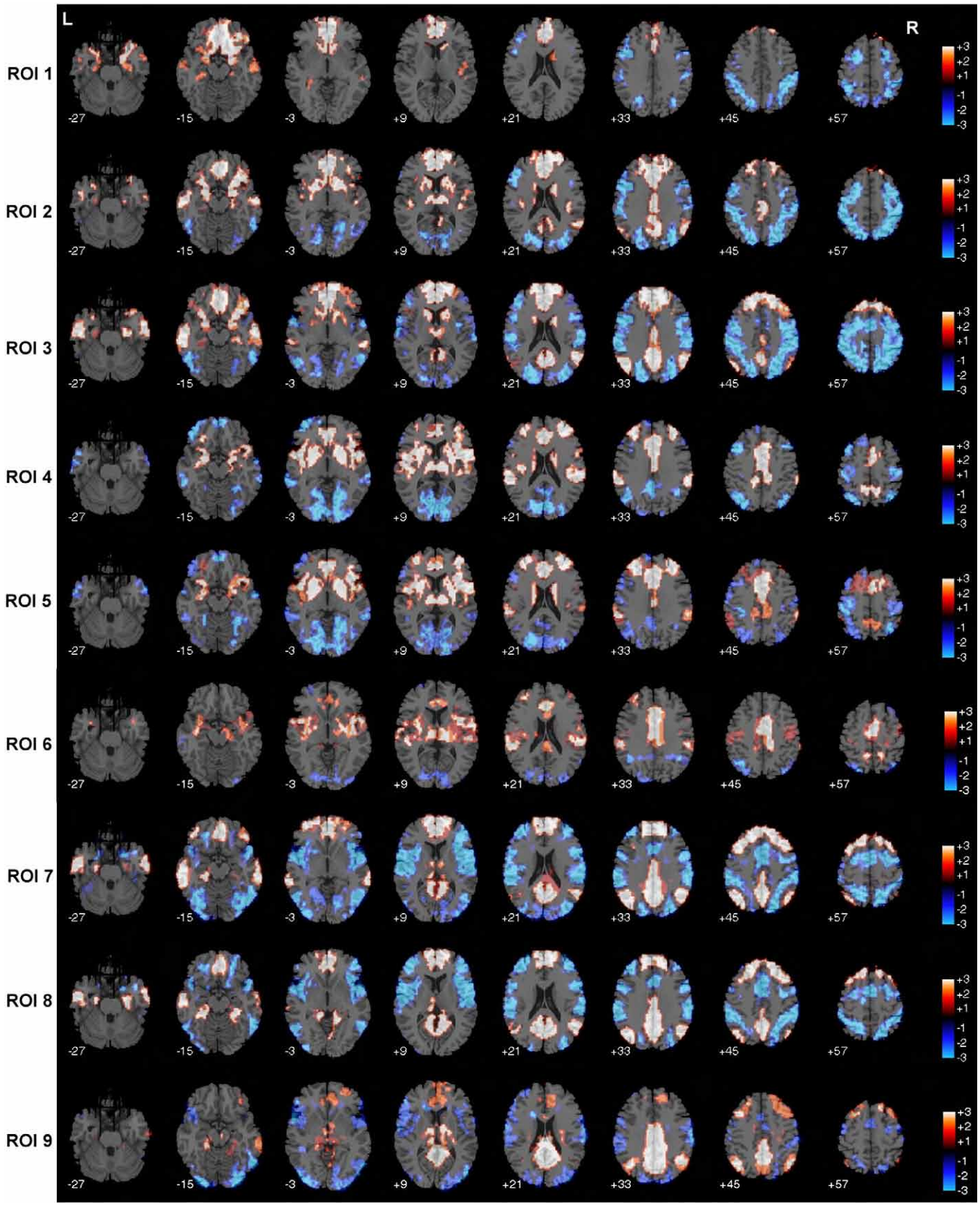

Fig. 2. Differences in the FC patterns between the left and right hemispheric ROIs. The FC maps of the left and right hemispheric ROIs are projected to the same structural background images to visualize the possible differences in the FC patterns between each pair of the ROIs. In the color bar, +1 represents the positive FC map of the left hemispheric ROI; +2 is the positive FC map of the right hemispheric ROI; +3 denotes the overlapping regions of the positive FC maps of the two hemispheric ROIs; −1 represents the negative FC map of the left hemispheric ROI; −2 is the negative FC map of the right hemispheric ROI; −3 denotes the overlapping regions of the negative FC maps of the two hemispheric ROIs. FC, functional connectivity; ROI, region of interest.

gradient echo (MP-RAGE) sequence (TR/TE = 2000/2.6 ms; FA = 9°; slice thickness = 1 mm, no gap).

Data preprocessing

Unless specially stated, all preprocessing steps were carried out using the statistical parametric mapping (SPM2, http://www.fil.ion.ucl.ac.uk/spm). The first 10 volumes of each functional time series were discarded for the magnetization equilibrium. The remaining 170 images were corrected for time delay between different slices and realigned to the first volume. Head motion parameters were computed by estimating the translation in each direction and the angular rotation on each axis for each volume, which provided a record of the head position. The realigned images were spatially normalized to the Montreal Neurological Institute (MNI) EPI template and re-sampled to 3 mm cubic voxel. The normalized images were smoothed with a Gaussian kernel of $6\times6\times6$ mm^3 full-width at half maximum.

The head motions of all subjects were less than the thresholds of 1.5 mm translation in each of the *x*, *y* and *z* directions and 1.5° rotation in each of the *x*, *y* and *z* axes. Since the FC analysis is sensitive to head motion, we further characterized the mean and peak displacements as measures of head motion (Jiang et al., 1995; Lowe et al., 1998). Several sources of spurious variances including the estimated motion parameters, linear drift, global average BOLD signals, and average BOLD signals in ventricular and white matter regions were removed from the data through linear regression (Fox et al., 2005; Greicius et al., 2003). Finally, temporal band-pass filtering (0.01 ~ 0.08 Hz) was performed on the time series of each voxel using AFNI (http://www.afni.nimh.nih.gov/) 3D Fourier program to reduce the effects of low-frequency drift and high-frequency noises (Fox et al., 2005; Lowe et al., 1998; Zhou et al., 2008). Anatomical images were obtained to visualize the results by averaging the normalized 3D T1-weighted images across all subjects.

Seed regions

Each cingulate cortex was divided into 7 subregions in both hemispheres. We extracted 9 regions of interest (ROIs) (Fig. 1) from the 7 subregions of each hemisphere according to the cytoarchitectural findings (Palomero-Gallagher et al., 2009; Vogt and Vogt, 2003; Vogt, 2005; Vogt et al., 2006). Every ROI was manually defined on the ch2bet structural template with the MRIcro software (www.mricro.com). Each ROI was smaller than the cytoarchitectural definition through marginal retractions in order to ensure the ROI within the corresponding cytoarchitectural area and to avoid crosstalk between every two adjacent ROIs. ROI 1 represents sACC (area 25), which was defined as the cortical area just below the genu of the corpus callosum. ROI 2 and ROI 3 represent the posterior (areas 24a, 24b, 24cv, 24cd) and anterior (area 32) parts of pACC. ROI 2 was defined as the anteroinferior 1/3 of area 24 with 5 mm retractions of the superior and inferior margins, respectively. ROI 3 was defined as the part of area 32 between the extension planes of the margins of ROI 2. ROI 4 and ROI 5 represent the inferior (areas a24a', a24b', 24c'v, 24c'd) and superior (area 32') parts of the aMCC. ROI 4 was defined as the part of the area 24 between two planes with 5 mm marginal retractions. The first plane is the coronal plane passing through the anterior commissure. The second plane is perpendicular to the area 24 passing through the intersectional line between the coronal plane through the anterior margin of the genu of the corpus callosum and the dorsal surface of area 24. ROI 5 was defined as the part of area 32' between the extension planes of the margins of ROI 4. ROI 6 represents the pMCC (areas p24a', p24b', 24dv, 24dd), which was defined as the part of area 24 between two coronal planes with marginal retractions of 3 mm. The first coronal plane passes through the anterior commissure, while the second coronal plane was obtained by 20 mm backward translation of the first plane (Vogt and Vogt, 2003). ROI 7 represents the dPCC (areas 23c, 23d, d23, 31), which was defined as the parts of areas 23 and 31 between two planes with anterior marginal retraction of 5 mm. One plane is the second coronal plane when defining the ROI 6. The other plane is an oblique coronal plane along the ventral branch of the splenial sulclus. ROI 8 represents the vPCC (areas v23, 31), which was defined as the parts of areas 23 and 31 below the second plane of ROI 7. ROI 9 represents the RSC (areas 29 and 30), which was defined as the central part of the ventral bank of the cingulate gyrus that is buried in the callosal sulcus between the anterior margin of the ROI 7 and the horizontal plane through the inferior margin of the splenium of the corpus callosum (Vogt et al., 2001, 2006). For all the ROIs, only gray matter voxels were extracted for functional connectivity analysis.

Functional connectivity analysis

For each subject, correlation coefficients between the mean time series of each seed region and that of each voxel of the whole brain were computed and then converted to *z* values using Fisher's *r*-to-*z* transformation to improve the normality. Then individuals' *z*-values were entered into a random effect one-sample *t*-test in a voxel-wise manner to determine brain regions that showed significant positive or negative correlations with the seed region. Due to the fact that the cerebellum was not entirely covered in all subjects and that the BOLD signals in white matter are suspicious, the statistical analyses were limited to a mask which is composed of the cerebral and sub-cortical regions in the AAL Atlas. Corrections for multiple comparisons were carried out by the false discovery rate (FDR) method with $p<0.05$ and cluster size > 50 voxels. Comparisons of FC maps between the left and right hemispheres of each ROI and between every two ROIs of each hemisphere were also provided.

Results

Differences in the FC patterns between the left and right hemispheric ROIs

For each pair of the 9 ROIs, we projected the FC maps of the left and right hemispheric ROIs to the same structural background images to visualize the possible differences in the FC patterns between each pair of the ROIs (Fig. 2). We found that the FC patterns of each pair of the two hemispheric ROIs were almost overlapped, which suggests that there were no obvious side differences between the two hemispheric ROIs. Additionally, there were small non-overlapping regions for each pair of the ROIs, which might be resulted from subtle differences in the location of each pair of ROIs and the individual variances of the cingulate cortex.

Positive FCs of cingulate subregions

The FC maps of each ROI were shown in Fig. S1–9 of the supplementary materials and the details were shown in Table S1 and S2 of the supplementary materials. The differences in the FC patterns between every two ROIs of each hemisphere were shown in Figs. 3–5 and Fig. S10–11 of the supplementary materials. The

Fig. 3. Differences in the FC patterns between every two ROIs (from ROI 1–2 to ROI 2–6) of the left hemisphere. The FC maps of every two ROIs are projected to the same structural background images to visualize the possible differences in the FC patterns between these two ROIs. In the color bar, +1 represents the positive FC map of the first ROI; +2 is the positive FC map of the second ROI; +3 denotes the overlapping regions of the positive FC maps of the two ROIs; −1 represents the negative FC map of the first ROI; −2 is the negative FC map of the second ROI; −3 denotes the overlapping regions of the negative FC maps of the two ROIs. Abbreviations: FC, functional connectivity; L, left; R, right; ROI, region of interest.

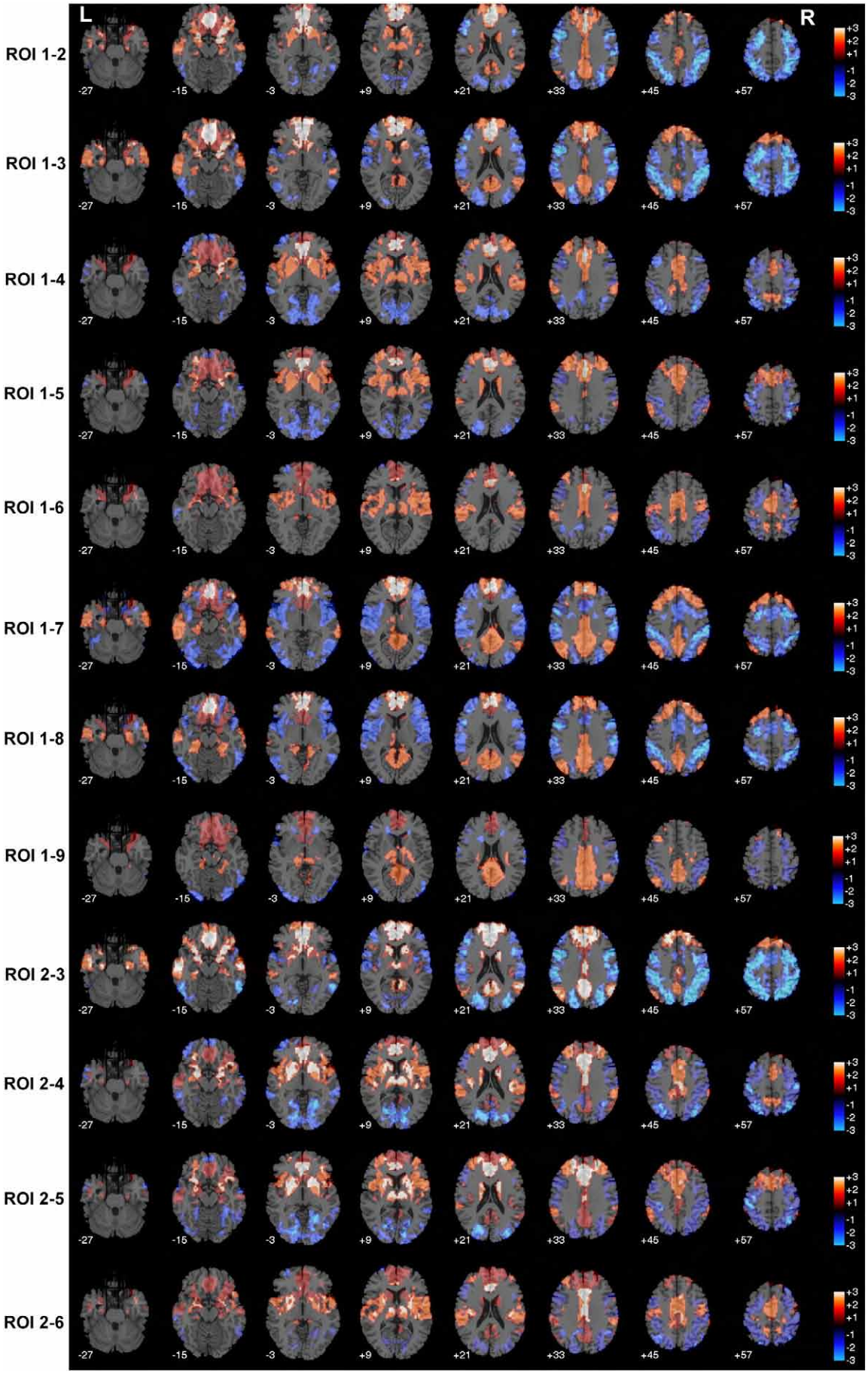
L
R
ROI 1-2
ROI 1-3
ROI 1-4
ROI 1-5
ROI 1-6
ROI 1-7
ROI 1-8
ROI 1-9
ROI 2-3
ROI 2-4
ROI 2-5
ROI 2-6
-27
-15
-3
+9
+21
+33
+45
+57
+3
+2
+1
-1
-2
-3

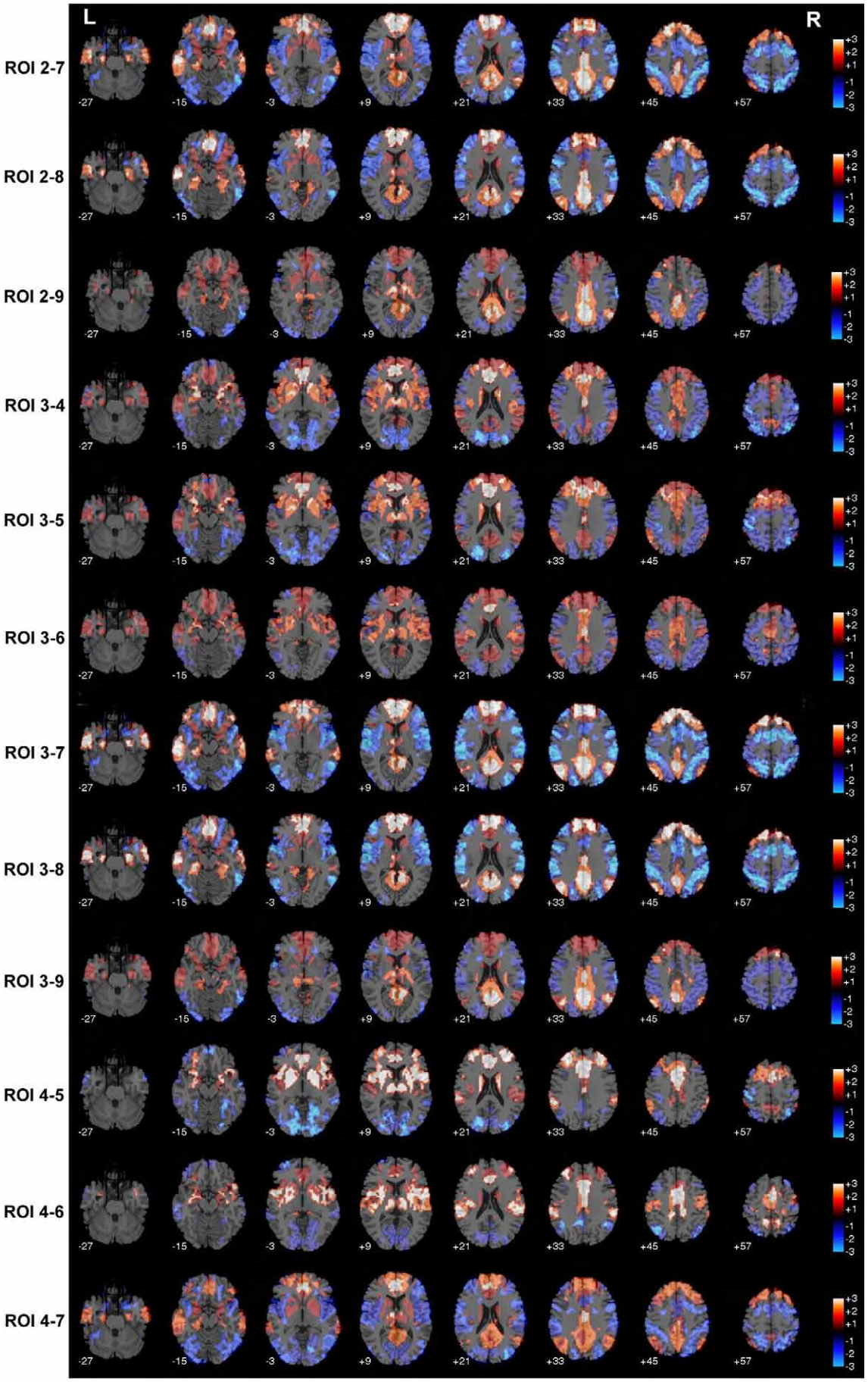
L
R
ROI 2-7
ROI 2-8
ROI 2-9
ROI 3-4
ROI 3-5
ROI 3-6
ROI 3-7
ROI 3-8
ROI 3-9
ROI 4-5
ROI 4-6
ROI 4-7
-27
-15
-3
+9
+21
+33
+45
+57
+3
+2
+1
-1
-2
-3

relationships between the 9 cingulate ROIs and the five functional networks were shown in Fig. 6.

The ROI 1 (sACC) mainly correlated with the AN including the MPFC, OFC and temporal pole. In contrast, the ROI 2 (pACC, area 24) correlated with more widespread brain areas belonging to different brain functional networks, such as the DMN, the AN, and brain regions that process different aspects of emotionally salient stimuli including amygdala and anterior insula, as well as other subcortical nuclei including the thalamus, caudate and putamen. The ROI 2 was also positively correlated with all other cingulate subregions (sACC, aMCC, pMCC, dPCC, vPCC and RSC). The ROI 3 (pACC, area 32) showed similar FC patterns to the ROI 2, which suggests the similar functions of these two ROIs.

The ROI 4 (aMCC, area 24) was positively correlated with the CN (DLPFC and dorsolateral parietal cortex), the salience network (fronto-insular cortex), the SMN (Rolandic area and SMA), and subcortical nuclei (thalamus, caudate, putamen, pallidum, and amygdala). The ROI 5 (aMCC, area 32') showed similar FC patterns to the ROI 4, but was correlated with more extensive DLPFC than that of the ROI 4. In contrast, the ROI 6 (pMCC) showed extensive FCs with the SMN including the PreCG, PostCG, ParaCG, Rolandic area, SMA, thalamus, superior marginal gyrus, and insula.

The ROI 7 (dPCC) and ROI 8 (vPCC) were positively correlated with the DMN including the bilateral PCC/Pcu, LPC, pACC/MPFC, anterior MTG/ITG, and anterior and medial parts of the SFG/MFG. In contrast, the ROI 9 (RSC) demonstrated positive FCs mainly with the PCC and the bilateral thalami. Although the right RSC also showed correlations with frontal, temporal and parietal regions belonging to the DMN, the spatial extent of the correlated regions and the strength of correlations were greatly less than those of the vPCC and dPCC.

Negative FCs of cingulate subregions

The ROI 1 (sACC) was anti-correlated with the SMN (PreCG and PostCG) and CN (DLPFC and dorsolateral parietal cortex). The ROI 2 (pACC, area 24) showed more extensive negative FCs with the SMN and CN than the sACC. In addition, the pACC was also anti-correlated with the VN including the SOG, MOG, calcarine cortex, cuneus lobe, lingual and fusiform gyri. The ROI 3 (pACC, area 32) showed similar anti-correlations to the ROI 2, but the spatial extent of the anti-correlated regions in the DMN and VN were larger than those of the ROI 2.

The ROI 4 (aMCC, area 24) was also anti-correlated with the VN (SOG, MOG, IOG, calcarine cortex, cuneus lobe, lingual and fusiform gyri), but in contrast to sACC and pACC, this ROI showed stronger anti-correlations to the DMN and AN (MPFC and OFC). The ROI 5 (aMCC, area 32') showed similar anti-correlations to those of the ROI 4. In contrast to aMCC, the ROI 6 (pMCC) showed negative FCs with the CN (DLPFC and dorsolateral parietal cortex) while it was similarly anti-correlated with the VN, but with a lesser extent.

Both ROI 7 (dPCC) and ROI 8 (vPCC) showed negative FCs with the VN (SOG, MOG, IOG, calcarine cortex, cuneus lobe, lingual and fusiform gyri), the SMN (PreCG/PostCG) and the CN (DLPFC and dorsolateral parietal cortex). In contrast, the ROI 9 (RSC) had similar patterns of the negative FCs to those of the vPCC and dPCC, but the spatial extent of the anti-correlated regions was larger in the VN but smaller in the SMN and CN than those of the PCC.

Discussion

In the present study, we systematically mapped the resting-state FC patterns of the human cingulate cortex for its anatomically and functionally predefined subregions (Vogt, 2005). Using a resting-state approach that is equally suitable for all functional partitions, we found that each cingulate subregion is specifically involved in different brain functional networks while anti-correlated to others.

The four-region model of the human cingulate cortex was proposed based on integrated neurobiological assessments (Vogt, 2005), and so far, it was a highly detailed and reasonable neurobiological model of this complex structure. In this model, the borders of each region are defined by anatomic markers, and a cortical region is an aggregate of areas that have a similar underlying cytoarchitectural motif, and common circuitry and functions (Vogt, 2005). This neurobiological model provides a basic framework for investigating structure and function of each cingulate subregion in healthy subjects, and for detecting structural and functional alterations of each subregion in diseased states. In the present study, we attempted to characterize the functional segregations and integrations of the predefined subregions in terms of FC patterns of the human cingulate cortex.

The main positively correlated brain regions with the sACC are the bilateral MPFC and OFC, which is in line with the finding that most cortical input to the sACC originated from the MPFC and OFC (Vogt and Pandya, 1987). Many task-based fMRI studies have shown that the sACC, MPFC, OFC and temporal pole were activated during sad events (George et al., 1995; Levesque et al., 2003; Pelletier et al., 2003), suggesting that they make up an affective network for processing negative emotional information. Thus, it seems that the sACC is a crucial node of the affective network, which is also supported by characteristic increases of baseline metabolism and connectivity in depressed patients (Botteron et al., 2002; Drevets et al., 1997; Greicius et al., 2007).

Consistent with most of the previous studies on the default-mode network (Fox et al., 2005; Fransson, 2005; Greicius et al., 2003), we found that the pACC showed positive FCs with brain regions belonging to the network, which supports the concept that the pACC is a core node of the DMN. Our finding suggests that the pACC is specifically involved in the affective network, which is in agreement with a number of relevant findings. The pACC is activated during pleasant and happy events, such as the warm and pleasant stimuli (Rolls et al., 2008), pleasant flavor (Grabenhorst et al., 2010), and making choices involving large gains (Grabenhorst et al., 2008; Rogers et al., 2004). Anhedonia, the inability to experience pleasure, was further related to functional and metabolite changes in this subregion in severely depressed patients (Walter et al., 2009). The activation of the pACC was however also associated with the degree of anxiety (Elsenbruch et al., 2010; Mobbs et al., 2009; Straube et al., 2009; Van Oudenhove et al., 2010) and in healthy volunteers the pACC was found important during regulation of emotional conflict on a trial-by-trial basis by dampening activity in the amygdala (Etkin et al., 2006) while this regulation may be disrupted in patients with generalized anxiety disorder (Etkin et al., 2010). It has been known that the pACC is also activated during noxious pain stimulations, especially the nociceptive visceral stimulations (Derbyshire et al., 1997; Matsuura et al., 2002; Strigo et al., 2003; Vogt, 2005), and is involved in pain control mechanism (Peyron et al., 2007; Zubieta et al., 2005). The importance of this cingulate subregion for affect regulation, integrating both features of automated regulation of bottom up information, mainly from amygdala, and top down control, from dorsal cognitive areas has also been extensively described in terms of clinical relevance for bipolar disorder (Phillips et al., 2008). Our findings of a specific integrative function of pACC also support this notion considering the

Fig. 4. Differences in the FC patterns between every two ROIs (from ROI 2–7 to ROI 4–7) of the left hemisphere. The FC maps of every two ROIs are projected to the same structural background images to visualize the possible differences in the FC patterns between these two ROIs. In the color bar, +1 represents the positive FC map of the first ROI; +2 is the positive FC map of the second ROI; +3 denotes the overlapping regions of the positive FC maps of the two ROIs; −1 represents the negative FC map of the first ROI; −2 is the negative FC map of the second ROI; −3 denotes the overlapping regions of the negative FC maps of the two ROIs. Abbreviations: FC, functional connectivity; L, left; R, right; ROI, region of interest.

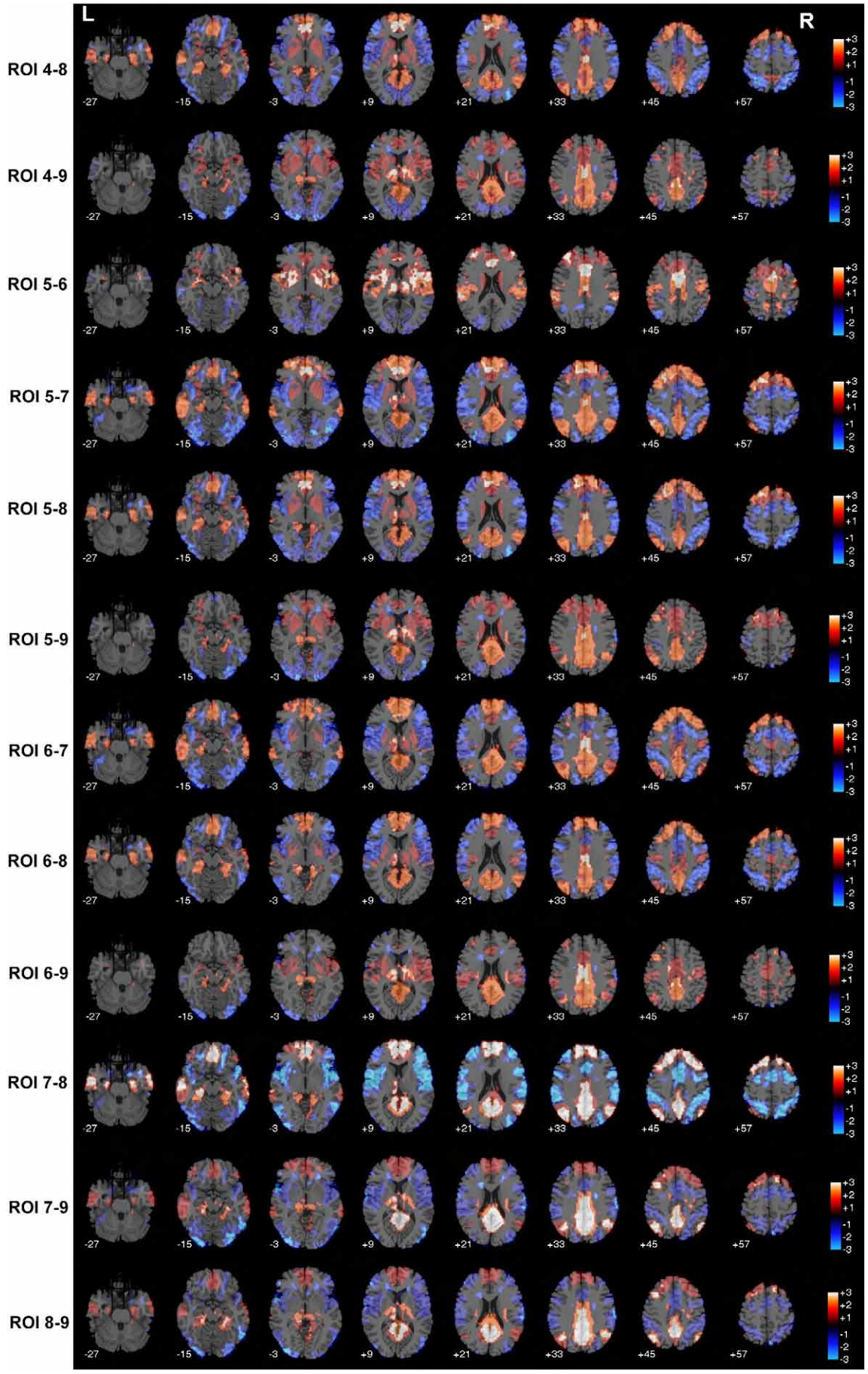
L
R
ROI 4-8
ROI 4-9
ROI 5-6
ROI 5-7
ROI 5-8
ROI 5-9
ROI 6-7
ROI 6-8
ROI 6-9
ROI 7-8
ROI 7-9
ROI 8-9
-27
-15
-3
+9
+21
+33
+45
+57
+3
+2
+1
-1
-2
-3

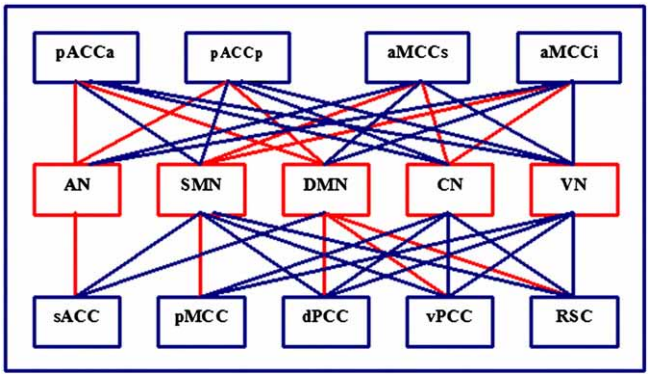

Fig. 6. Relationships between the 9 cingulate ROIs and the five functional networks. The red line represents positive correlation between the connected ROI and functional network, while the blue line denotes anti-correlation between the connected ROI and functional network. Abbreviations: AN, affective network; aMCCi, inferior part of the anterior midcingulate cortex; aMCCs, superior part of the anterior midcingulate cortex; CN, cognitive network; DMN, default-mode network; dPCC, dorsal part of the posterior cingulate cortex; pACCa, anterior part of the pregenual anterior cingulate cortex; pACCp, posterior part of the pregenual anterior cingulate cortex; pMCC, posterior midcingulate cortex; RSC, retrosplenial cortex; sACC, subgenual anterior cingulate cortex; SMN, sensorimotor network; VN, visual network; vPCC, ventral part of the posterior cingulate cortex.

extensive connectivities with other affective and cognitive related cortical and subcortical networks, including the insula, thalamus, caudate and putamen. In further support of its central role, the pACC is the only cingulate subregion who connected with every other cingulate subregions, through which information can be exchanged between the affective (sACC), cognitive (aMCC), sensorimotor (pMCC), and the default-mode (PCC and RSC) networks. Reflecting its central position in the rostro-caudal continuum of the cingulate cortex our findings may thus support the role of pACC as the anterior cingulate association area, as opposed to other more specialized cingulate regions that is crucial for cognitive emotional interaction and conscious self-reflection in higher primates and humans. When we further divided the pACC into ROI 2 (area 24) and ROI 3 (area 32), the FC patterns were similar to each other. This supports the validity of the four-region model which categorized these two areas into a region of the pACC.

We found that the aMCC positively connected with the DLPFC, which is consistent with the anatomic finding of the reciprocal connections between these two brain regions (Barbas and Pandya, 1989; Bates and Goldmanrakic, 1993). This is also supported by the findings that the aMCC is activated during a variety of cognitive tasks including conflict monitoring (Sohn et al., 2007; Ursu et al., 2009), error detection (Gehring and Fencsik, 2001; Pourtois et al., 2010), response selection (Awh and Gehring, 1999; Paus, 2001), and attention control (Crottaz-Herbette and Menon, 2006; Luo et al., 2007). The positive FC between the aMCC and SMA may be explained by strong contributions of the rostral cingulate motor area located in the aMCC, which is mainly connected with dorsal premotor area and pre-SMA (Hatanaka et al., 2003), and which is activated during the complex motor tasks (Picard and Strick, 1996). The aMCC receives dense projection of nociceptive inputs from the thalamus (Hatanaka et al., 2003), and is activated during pain stimulations (Vogt, 2005), which can explain the positive FCs between these regions. Additionally, we found strong FCs between aMCC and insula, which is in agreement with prior resting-state fMRI studies on the resting-state network (Seeley et al., 2007; Taylor et al., 2009). Both of these two structures are the core regions of the salience network, which underlie interoceptive-autonomic processing (Critchley, 2005; Downar et al., 2002). Taken all together, we suggest that the aMCC is a central node for willed control of behaviors (Paus, 2001) based on its characteristic connections with sensorimotor, cognitive, salience, pain and affective networks. Area 32' is a new brain region in human cingulate cortex that is not present in monkeys (Cole et al., 2009; Palomero-Gallagher et al., 2008; Vogt et al., 1995). Thus we divided the aMCC into ROI 4 (area 24) and ROI 5 (area 32'), the FC patterns of these two ROIs were similar, but the 32' was correlated with more extensive DLPFC than that of the ROI 4 (area 24). This finding supports the notion that human area 32' bestows mental flexibility on humans, improving our ability to perform well on a variety of tasks (Cole et al., 2009, 2010).

In line with previous resting-state FC studies (Habas, 2010; Margulies et al., 2007; Taylor et al., 2009), the pMCC showed extensively FCs with brain regions that belonged to the sensorimotor network, which is consistent with its function in processing simple motor tasks (Picard and Strick, 1996) and its connections with the primary motor cortex and spinal cord (Dum and Strick, 1991). The pMCC connected with the bilateral thalami through which the spinothalamic input access this subregion (Dum et al., 2009), which underlies the activation of the pMCC during noxious thermal skin stimulations (Vogt, 2005). Thus it seems that the main function of the pMCC is involved in the processing of motor and pain.

Although the functions of the dPCC and vPCC are different in that the former is mainly involved in spatial processing (Vogt et al., 2006), but the latter is involved in self-referential processing (Northoff and Bermpohl, 2004; Vogeley et al., 2001), the FC patterns are very similar. Both of these two cingulate subregions were mainly correlated with the DMN, which suggests that both of these two brain areas can be used to construct the DMN. In contrast, similar to a previous PET study (Vogt et al., 2006), the RSC was mainly correlated with the bilateral thalami and PCC, which is consistent with anatomic findings of heavy connections between RSC and thalamus (Kobayashi and Amaral, 2003, 2007), and between RSC and adjacent area 23 (Vogt and Pandya, 1987). The differences in the FC patterns between the RSC and PCC support that they are two different cingulate subregions and further validate the validity of the four-region model of the human cingulate cortex. However, we also found weak but significant FCs between the right RSC and frontal, parietal and temporal areas belonging to the DMN. This unexpected finding is more likely caused by the contamination of the ROI 9 by the adjacent area 23 (a part of the PCC), which is the core node of the DMN. This contamination is related to the mismatching of the cortical thickness of the RSC (2–4 mm) and the poor resolution ($3.4\times3.4\times4.0$ mm) of the fMRI scans, smoothing with a Gaussian kernel of $6\times6\times6$ mm^3 full-width at half maximum, the individual variability of the shape and location of the RSC, and so on. Thus one should be cautious when interpreting the result of significant FC between RSC and the DMN.

Anti-correlations were also found between each cingulate subregion and different brain functional networks, which is consistent with previous findings of anti-correlations between task-positive network and the default-mode network (Fox et al., 2005; Greicius et al., 2003; Tian et al., 2007; Zhou et al., 2010) and between neural systems underlying different components of verbal working memory(Gruber et al., 2007). Greicius et al. (2003) suggested that intrinsic anti-correlated activity might relate to the differential task-related responses in these regions (Greicius et al., 2003). Fox et al. (2005) proposed that

Fig. 5. Differences in the FC patterns between every two ROIs (from ROI 4–8 to ROI 8–9) of the left hemisphere. The FC maps of every two ROIs are projected to the same structural background images to visualize the possible differences in the FC patterns between these two ROIs. In the color bar, +1 represents the positive FC map of the first ROI; +2 is the positive FC map of the second ROI; +3 denotes the overlapping regions of the positive FC maps of the two ROIs; −1 represents the negative FC map of the first ROI; −2 is the negative FC map of the second ROI; −3 denotes the overlapping regions of the negative FC maps of the two ROIs. Abbreviations: FC, functional connectivity; L, left; R, right; ROI, region of interest.

anti-correlations may serve as a differentiating role in segregating neuronal processes subserving opposite goals or competing representations (Fox et al., 2005). In the present study, anti-correlations showed three features: (1) seed region and anti-correlated brain regions have different functions; (2) anti-correlations do not exist in all the functionally different brain networks but show a highly specific or selective distribution; (3) each cingulate subregion has its specific anti-correlated networks even if subregions (pACC, dPCC and vPCC) belong to the same default-mode network, which is supported by Uddin et al. (2009). Based on the above-mentioned findings, we suggest that each cingulate subregion correlated and anti-correlated with specific brain networks, which may facilitate its involved functioning while inhibiting other competing function systems. However, one should be cautious when interpreting anti-correlations derived from the resting-state fMRI studies since it remains an unsettled debate on whether the anti-correlation is an artifact of the global signal regression (Murphy et al., 2009; Weissenbacher et al., 2009) or reflects dynamic, anti-correlated functional networks (Hampson et al., 2010).

There are methodologic limitations of the current study that should be considered when interpreting our results. Firstly, we cannot guarantee that the actual location of each cingulate subregion was absolutely the same across subjects. Secondly, we did not include the cerebellum in the FC analysis because it was not completely covered in all subjects. Finally, we cannot exclude the influence of physiological noise because of a relatively low sampling rate (2s) for multi-slice acquisitions. Under this sampling rate, respiratory and cardiac fluctuations may be present in the time series data (Lowe et al., 1998). We used a band-pass filtering of 0.01–0.08 Hz to partly reduce these physiological noises. However, the filtering cannot eliminate them completely. Moreover, subtle changes in a subject's breathing rate or depth, which occur naturally during rest at low frequencies (<0.1 Hz), have been shown to be correlated with fMRI signal changes throughout gray matter (Birn et al., 2006; Wise et al., 2004). As these authors (Birn et al., 2006) suggested, we cued the subjects to breathe at a relatively constant rate and depth and regressed out global signal changes to reduce such effects.

In conclusion, we here reported the first attempt to our knowledge to validate the validity of the four-region model of the human cingulate cortex from the perspective of functional connectivity. Applying a resting state fMRI approach to anatomically predefined cingulate subregions, we found that each cingulate subregion was specifically correlated and anti-correlated with a set of brain functional networks, which confirms the validity of the four region model of the human cingulate cortex and the hypotheses generated by functional and neuroanatomical studies which put the cingulate cortex into a central position during integration of sensorimotor, cognitive and affective information.

Acknowledgments

This work was supported by the National Basic Research Program of China (973 program, No. 2011CB707801), the Natural Science Foundation of China (Nos. 30870694, 30900487 and 30730036), the Program for New Century Excellent Talents in University (NCET-07-0568), and the SFB 779 to MW.

Appendix A. Supplementary data

Supplementary data to this article can be found online at doi:10.1016/j.neuroimage.2010.11.018.

References

Awh, E., Gehring, W.J., 1999. The anterior cingulate cortex lends a hand in response selection. Nat. Neurosci. 2, 853–854.
Barbas, H., Pandya, D.N., 1989. Architecture and intrinsic connections of the prefrontal cortex in the Rhesus-monkey. J. Comp. Neurol. 286, 353–375.
Bates, J.F., Goldmanrakic, P.S., 1993. Prefrontal connections of medial motor areas in the Rhesus-monkey. J. Comp. Neurol. 336, 211–228.
Beckmann, M., Johansen-Berg, H., Rushworth, M.F.S., 2009. Connectivity-based parcellation of human cingulate cortex and its relation to functional specialization. J. Neurosci. 29, 1175–1190.
Birn, R.M., Diamond, J.B., Smith, M.A., Bandettini, P.A., 2006. Separating respiratory-variation-related neuronal-activity-related fluctuations in fluctuations from fMRI. Neuroimage 31, 1536–1548.
Botteron, K.N., Raichle, M.E., Drevets, W.C., Heath, A.C., Todd, R.D., 2002. Volumetric reduction in left subgenual prefrontal cortex in early onset depression. Biol. Psychiatry 51, 342–344.
Cole, M.W., Yeung, N., Freiwald, W.A., Botvinick, M., 2009. Cingulate cortex: diverging data from humans and monkeys. Trends Neurosci. 32, 566–574.
Cole, M.W., Yeung, N., Freiwald, W.A., Botvinick, M., 2010. Conflict over cingulate cortex: between-species differences in cingulate may support enhanced cognitive flexibility in humans. Brain Behav. Evol. 75, 239–240.
Critchley, H.D., 2005. Neural mechanisms of autonomic, affective, and cognitive integration. J. Comp. Neurol. 493, 154–166.
Crottaz-Herbette, S., Menon, V., 2006. Where and when the anterior cingulate cortex modulates attentional response: combined fMRI and ERP evidence. J. Cogn. Neurosci. 18, 766–780.
Derbyshire, S.W.G., Jones, A.K.P., Gyulai, F., Clark, S., Townsend, D., Firestone, L.L., 1997. Pain processing during three levels of noxious stimulation produces differential patterns of central activity. Pain 73, 431–445.
Downar, J., Crawley, A.P., Mikulis, D.J., Davis, K.D., 2002. A cortical network sensitive to stimulus salience in a neutral behavioral context across multiple sensory modalities. J. Neurophysiol. 87, 615–620.
Drevets, W.C., Price, J.L., Simpson, J.R., Todd, R.D., Reich, T., Vannier, M., Raichle, M.E., 1997. Subgenual prefrontal cortex abnormalities in mood disorders. Nature 386, 824–827.
Dum, R.P., Strick, P.L., 1991. The origin of corticospinal projections from the premotor areas in the frontal-lobe. J. Neurosci. 11, 667–689.
Dum, R.P., Levinthal, D.J., Strick, P.L., 2009. The spinothalamic system targets motor and sensory areas in the cerebral cortex of monkeys. J. Neurosci. 29, 14223–14235.
Elsenbruch, S., Rosenberger, C., Enck, P., Forsting, M., Schedlowski, M., Gizewski, E.R., 2010. Affective disturbances modulate the neural processing of visceral pain stimuli in irritable bowel syndrome: an fMRI study. Gut 59, 489–495.
Enzi, B., de Greck, M., Prosch, U., Tempelmann, C., Northoff, G., 2009. Is our self nothing but reward? neuronal overlap and distinction between reward and personal relevance and its relation to human personality. PLoS ONE 4.
Etkin, A., Egner, T., Peraza, D.M., Kandel, E.R., Hirsch, J., 2006. Resolving emotional conflict: a role for the rostral anterior cingulate cortex in modulating activity in the amygdala. Neuron 51, 871–882.
Etkin, A., Prater, K.E., Hoeft, F., Menon, V., Schatzberg, A.F., 2010. Failure of anterior cingulate activation and connectivity with the amygdala during implicit regulation of emotional processing in generalized anxiety disorder. Am. J. Psychiatry 167, 545–554.
Fink, G.R., Halligan, P.W., Marshall, J.C., Frith, C.D., Frackowiak, R.S.J., Dolan, R.J., 1997. Neural mechanisms involved in the processing of global and local aspects of hierarchically organized visual stimuli. Brain 120, 1779–1791.
Fox, M.D., Snyder, A.Z., Vincent, J.L., Corbetta, M., Van Essen, D.C., Raichle, M.E., 2005. The human brain is intrinsically organized into dynamic, anticorrelated functional networks. Proc. Natl Acad. Sci. USA 102, 9673–9678.
Fransson, P., 2005. Spontaneous low-frequency BOLD signal fluctuations: an fMRI investigation of the resting-state default mode of brain function hypothesis. Hum. Brain Mapp. 26, 15–29.
Friston, K.J., Holmes, A., Poline, J.B., Price, C.J., Frith, C.D., 1996. Detecting activations in PET and fMRI: levels of inference and power. Neuroimage 4, 223–235.
Gehring, W.J., Fencsik, D.E., 2001. Functions of the medial frontal cortex in the processing of conflict and errors. J. Neurosci. 21, 9430–9437.
George, M.S., Ketter, T.A., Parekh, P.I., Horwitz, B., Herscovitch, P., Post, R.M., 1995. Brain activity during transient sadness and happiness in healthy women. Am. J. Psychiatry 152, 341–351.
Grabenhorst, F., Rolls, E.T., Parris, B.A., 2008. From affective value to decision-making in the prefrontal cortex. Eur. J. Neurosci. 28, 1930–1939.
Grabenhorst, F., Rolls, E.T., Parris, B.A., d'Souza, A.A., 2010. How the brain represents the reward value of fat in the mouth. Cereb. Cortex 20, 1082–1091.
Greicius, M.D., Krasnow, B., Reiss, A.L., Menon, V., 2003. Functional connectivity in the resting brain: a network analysis of the default mode hypothesis. Proc. Natl Acad. Sci. USA 100, 253–258.
Greicius, M.D., Flores, B.H., Menon, V., Glover, G.H., Solvason, H.B., Kenna, H., Reiss, A.L., Schatzberg, A.F., 2007. Resting-state functional connectivity in major depression: abnormally increased contributions from subgenual cingulate cortex and thalamus. Biol. Psychiatry 62, 429–437.
Gruber, O., Muller, T., Falkai, P., 2007. Dynamic interactions between neural systems underlying different components of verbal working memory. J. Neural Transm. 114, 1047–1050.
Habas, C., 2010. Functional connectivity of the human rostral and caudal cingulate motor areas in the brain resting state at 3T. Neuroradiology 52, 47–59.
Hampson, M., Driesen, N., Roth, J.K., Gore, J.C., Constable, R.T., 2010. Functional connectivity between task-positive and task-negative brain areas and its relation to working memory performance. Magn. Reson. Imaging 28, 1051–1057.
Hanggi, J., Koeneke, S., Bezzola, L., Jancke, L., 2010. Structural neuroplasticity in the sensorimotor network of professional female ballet dancers. Hum. Brain Mapp. 31, 1196–1206.
Hatanaka, N., Tokuno, H., Hamada, I., Inase, M., Ito, Y., Imanishi, M., Hasegawa, N., Akazawa, T., Nambu, A., Takada, M., 2003. Thalamocortical and intracortical connections of monkey cingulate motor areas. J. Comp. Neurol. 462, 121–138.

Jiang, A.P., Kennedy, D.N., Baker, J.R., Weisskoff, R.M., Tootell, R.B.H., Woods, R.P., Benson, R.R., Kwong, K.K., Brady, T.J., Rosen, B.R., Belliveau, J.W., 1995. Motion detection and correction in functional MR imaging. Hum. Brain Mapp. 3, 224–235.
Keisker, B., Hepp-Reymond, M.C., Blickenstorfer, A., Kollias, S.S., 2010. Differential representation of dynamic and static power grip force in the sensorimotor network. Eur. J. Neurosci. 31, 1483–1491.
Kelley, W.M., Macrae, C.N., Wyland, C.L., Caglar, S., Inati, S., Heatherton, T.F., 2002. Finding the self? An event-related fMRI study. J. Cogn. Neurosci. 14, 785–794.
Kobayashi, Y., Amaral, D.G., 2003. Macaque monkey retrosplenial cortex: II. Cortical afferents. J. Comp. Neurol. 466, 48–79.
Kobayashi, Y., Amaral, D.G., 2007. Macaque monkey retrosplenial cortex: III. Cortical efferents. J. Comp. Neurol. 502, 810–833.
Kross, E., Davidson, M., Weber, J., Ochsner, K., 2009. Coping with emotions past: the neural bases of regulating affect associated with negative autobiographical memories. Biol. Psychiatry 65, 361–366.
Levesque, J., Joanette, Y., Mensour, B., Beaudoin, G., Leroux, J.M., Bourgouin, P., Beauregard, M., 2003. Neural correlates of sad feelings in healthy girls. Neuroscience 121, 545–551.
Liotti, M., Mayberg, H.S., Brannan, S.K., McGinnis, S., Jerabek, P., Fox, P.T., 2000. Differential limbic-cortical correlates of sadness and anxiety in healthy subjects: implications for affective disorders. Biol. Psychiatry 48, 30–42.
Lowe, M.J., Mock, B.J., Sorenson, J.A., 1998. Functional connectivity in single and multislice echoplanar imaging using resting-state fluctuations. Neuroimage 7, 119–132.
Luo, Q., Mitchell, D., Jones, M., Mondillo, K., Vythilingam, M., Blair, R.J., 2007. Common regions of dorsal anterior cingulate and prefrontal-parietal cortices provide attentional control of distracters varying in emotionality and visibility. Neuroimage 38, 631–639.
Maguire, E.A., 2001. The retrosplenial contribution to human navigation: a review of lesion and neuroimaging findings. Scand. J. Psychol. 42, 225–238.
Margulies, D.S., Kelly, A.M.C., Uddin, L.Q., Biswal, B.B., Castellanos, F.X., Milham, M.P., 2007. Mapping the functional connectivity of anterior cingulate cortex. Neuroimage 37, 579–588.
Matsuura, S., Kakizaki, H., Mitsui, T., Shiga, T., Tamaki, N., Koyanagi, T., 2002. Human brain region response to distention or cold stimulation of the bladder: a positron emission tomography study. J. Urol. 168, 2035–2039.
Mobbs, D., Marchant, J.L., Hassabis, D., Seymour, B., Tan, G., Gray, M., Petrovic, P., Dolan, R.J., Frith, C.D., 2009. From threat to fear: the neural organization of defensive fear systems in humans. J. Neurosci. 29, 12236–12243.
Murphy, K., Birn, R.M., Handwerker, D.A., Jones, T.B., Bandettini, P.A., 2009. The impact of global signal regression on resting state correlations: are anti-correlated networks introduced? Neuroimage 44, 893–905.
Northoff, G., Bermpohl, F., 2004. Cortical midline structures and the self. Trends Cogn. Sci. 8, 102–107.
Oldfield, R.C., 1971. The assessment and analysis of handedness: the Edinburgh inventory. Neuropsychologia 9, 97–113.
Palomero-Gallagher, N., Mohlberg, H., Zilles, K., Vogt, B., 2008. Cytology and receptor architecture of human anterior cingulate cortex. J. Comp. Neurol. 508, 906–926.
Palomero-Gallagher, N., Vogt, B.A., Schleicher, A., Mayberg, H.S., Zilles, K., 2009. Receptor architecture of human cingulate cortex: evaluation of the four-region neurobiological model. Hum. Brain Mapp. 30, 2336–2355.
Paus, T., 2001. Primate anterior cingulate cortex: where motor control, drive and cognition interface. Nat. Rev. Neurosci. 2, 417–424.
Pelletier, M., Bouthillier, A., Levesque, J., Carrier, S., Breault, C., Paquette, V., Mensour, B., Leroux, J.M., Beaudoin, G., Bourgouin, P., Beauregard, M., 2003. Separate neural circuits for primary emotions? Brain activity during self-induced sadness and happiness in professional actors. NeuroReport 14, 1111–1116.
Peyron, R., Faillenot, I., Mertens, P., Laurent, B., Garcia-Larrea, L., 2007. Motor cortex stimulation in neuropathic pain. Correlations between analgesic effect and hemodynamic changes in the brain. A PET study. Neuroimage 34, 310–321.
Phillips, M., Ladouceur, C., Drevets, W., 2008. A neural model of voluntary and automatic emotion regulation: implications for understanding the pathophysiology and neurodevelopment of bipolar disorder. Mol. Psychiatry 13, 833–857.
Picard, N., Strick, P.L., 1996. Motor areas of the medial wall: a review of their location and functional activation. Cereb. Cortex 6, 342–353.
Picard, N., Strick, P.L., 2001. Imaging the premotor areas. Curr. Opin. Neurobiol. 11, 663–672.
Pourtois, G., Vocat, R., N'Diaye, K., Spinelli, L., Seeck, M., Vuilleumier, P., 2010. Errors recruit both cognitive and emotional monitoring systems: simultaneous intracranial recordings in the dorsal anterior cingulate gyrus and amygdala combined with fMRI. Neuropsychologia 48, 1144–1159.
Rogers, R.D., Ramnani, N., Mackay, C., Wilson, J.L., Jezzard, P., Carter, C.S., Smith, S.M., 2004. Distinct portions of anterior cingulate cortex and medial prefrontal cortex are activated by reward processing in separable phases of decision-making cognition. Biol. Psychiatry 55, 594–602.
Rolls, E.T., Grabenhorst, F., Parris, B.A., 2008. Warm pleasant feelings in the brain. Neuroimage 41, 1504–1513.
Seeley, W.W., Menon, V., Schatzberg, A.F., Keller, J., Glover, G.H., Kenna, H., Reiss, A.L., Greicius, M.D., 2007. Dissociable intrinsic connectivity networks for salience processing and executive control. J. Neurosci. 27, 2349–2356.
Sohn, M.H., Albert, M.V., Jung, K.J., Carter, C.S., Anderson, J.R., 2007. Anticipation of conflict monitoring in the anterior cingulate cortex and the prefrontal cortex. Proc. Natl Acad. Sci. USA 104, 10330–10334.
Straube, T., Schmidt, S., Weiss, T., Mentzel, H.J., Miltner, W.H.R., 2009. Dynamic activation of the anterior cingulate cortex during anticipatory anxiety. Neuroimage 44, 975–981.
Strigo, I.A., Duncan, G.H., Boivin, M., Bushnell, M.C., 2003. Differentiation of visceral and cutaneous pain in the human brain. J. Neurophysiol. 89, 3294–3303.
Taylor, K.S., Seminowicz, D.A., Davis, K.D., 2009. Two systems of resting state connectivity between the insula and cingulate cortex. Hum. Brain Mapp. 30, 2731–2745.
Tian, L.X., Jiang, T.Z., Liu, Y., Yu, C.S., Wang, K., Zhou, Y., Song, M., Li, K.C., 2007. The relationship within and between the extrinsic and intrinsic systems indicated by resting state correlational patterns of sensory cortices. Neuroimage 36, 684–690.
Uddin, L.Q., Kelly, A.M., Biswal, B.B., Xavier Castellanos, F., Milham, M.P., 2009. Functional connectivity of default mode network components: correlation, anticorrelation, and causality. Hum. Brain. Mapp. 30, 625–637.
Ursu, S., Clark, K.A., Aizenstein, H.J., Stenger, V.A., Carter, C.S., 2009. Conflict-related activity in the caudal anterior cingulate cortex in the absence of awareness. Biol. Psychol. 80, 279–286.
van den Heuvel, M.P., Pol, H.E.H., 2010. Exploring the brain network: a review on resting-state fMRI functional connectivity. Eur. Neuropsychopharmacol. 20, 519–534.
Van Oudenhove, L., Vandenberghe, J., Dupont, P., Geeraerts, B., Vos, R., Dirix, S., Bormans, G., Vanderghinste, D., Van Laere, K., Demyttenaere, K., Fischler, B., Tack, J., 2010. Abnormal regional brain activity during rest and (anticipated) gastric distension in functional dyspepsia and the role of anxiety: a (H2O)-O-15-PET study. Am. J. Gastroenterol. 105, 913–924.
Vann, S.D., Aggleton, J.P., Maguire, E.A., 2009. What does the retrosplenial cortex do? Nat. Rev. Neurosci. 10, 792–802.
Vogeley, K., Bussfeld, P., Newen, A., Herrmann, S., Happe, F., Falkai, P., Maier, W., Shah, N.J., Fink, G.R., Zilles, K., 2001. Mind reading: neural mechanisms of theory of mind and self-perspective. Neuroimage 14, 170–181.
Vogt, B.A., 2005. Pain and emotion interactions in subregions of the cingulate gyrus. Nat. Rev. Neurosci. 6, 533–544.
Vogt, B.A., Pandya, D.N., 1987. Cingulate cortex of the Rhesus-Monkey.2. Cortical afferents. J. Comp. Neurol. 262, 271–289.
Vogt, B.A., Vogt, L., 2003. Cytology of human dorsal midcingulate and supplementary motor cortices. J. Chem. Neuroanat. 26, 301–309.
Vogt, B.A., Sikes, R.W., Vogt, L.J., 1993. In: Vogt, B.A., Gabriel, M. (Eds.), Neurobiology of Cingulate Cortex and Limbic Thalamus. Birkhäuser, Boston, pp. 19–70. 313-344.
Vogt, B.A., Nimchinsky, E.A., Vogt, L.J., Hof, P.R., 1995. Human cingulate cortex: surface features, flat maps, and cytoarchitecture. J. Comp. Neurol. 359, 490–506.
Vogt, B.A., Vogt, L.J., Perl, D.P., Hof, P.R., 2001. Cytology of human caudomedial cingulate, retrosplenial, and caudal parahippocampal cortices. J. Comp. Neurol. 438, 353–376.
Vogt, B.A., Vogt, L., Laureys, S., 2006. Cytology and functionally correlated circuits of human posterior cingulate areas. Neuroimage 29, 452–466.
Walter, M., Bermpohl, F., Mouras, H., Schiltz, K., Tempelmann, C., Rotte, M., Heinze, H.J., Bogerts, B., Northoff, G., 2008. Distinguishing specific sexual and general emotional effects in fMRI-subcortical and cortical arousal during erotic picture viewing. Neuroimage 40, 1482–1494.
Walter, M., Henning, A., Grimm, S., Schulte, R.F., Beck, J., Dydak, U., Schnepf, B., Boeker, H., Boesiger, P., Northoff, G., 2009. The relationship between aberrant neuronal activation in the pregenual anterior cingulate, altered glutamatergic metabolism, and anhedonia in major depression. Arch. Gen. Psychiatry 66, 478–486.
Weissenbacher, A., Kasess, C., Gerstl, F., Lanzenberger, R., Moser, E., Windischberger, C., 2009. Correlations and anticorrelations in resting-state functional connectivity MRI: a quantitative comparison of preprocessing strategies. Neuroimage 47, 1408–1416.
Wise, R.G., Ide, K., Poulin, M.J., Tracey, I., 2004. Resting fluctuations in arterial carbon dioxide induce significant low frequency variations in BOLD signal. Neuroimage 21, 1652–1664.
Zhou, Y., Shu, N., Liu, Y., Song, M., Hao, Y., Liu, H., Yu, C., Liu, Z., Jiang, T., 2008. Altered resting-state functional connectivity and anatomical connectivity of hippocampus in schizophrenia. Schizophr. Res. 100, 120–132.
Zhou, Y., Yu, C., Zheng, H., Liu, Y., Song, M., Qin, W., Li, K., Jiang, T., 2010. Increased neural resources recruitment in the intrinsic organization in major depression. J. Affect. Disord. 121, 220–230.
Zubieta, J.K., Bueller, J.A., Jackson, L.R., Scott, D.J., Xu, Y., Koeppe, R.A., Nichols, T.E., Stohler, C.S., 2005. Placebo effects mediated by endogenous opioid activity on mu-opioid receptors. J. Neurosci. 25, 7754–7762.